Chinese Chemical Letters 34 (2023) 107832

Contents lists available at ScienceDirect

Chinese Chemical Letters

journal homepage: www.elsevier.com/locate/cclet

# Pre-constructed SEI on graphite-based interface enables long cycle stability for dual ion sodium batteries

Bao Li, Bobo Cao, Xinxin Zhou, Zhuangzhuang Zhang, Dongmei Dai*, Mengmin Jia*, Dai-Huo Liu*

*Collaborative Innovation Center of Henan Province for Green Manufacturing of Fine Chemicals, Key Laboratory of Green Chemical Media and Reactions, Ministry of Education, School of Chemistry and Chemical Engineering, Henan Normal University, Xinxiang 453007, China*

ARTICLE INFO

*Article history:*
Received 21 June 2022
Revised 8 August 2022
Accepted 14 September 2022
Available online 17 September 2022

*Keywords:*
Dual ion sodium batteries
Carbonate electrolyte
High voltage
Anion co-intercalation
Pre-constructed SEI

ABSTRACT

Lithium batteries have been widely used in all over the world for its high energy density, long-term cycle stability. While the resources of lithium metal and transition metal are limited, which restrict their applications in the grid energy storage. Dual ion sodium batteries (DISBs) possess higher energy density, especially owning high power density for its higher operating voltage (> 4.5 V). Nevertheless, the poor oxidation tolerance of carbonate electrolyte and the co-intercalation of solvents accompanied with anions are main obstacles to make the DISBs commercialization. Herein, a physical barrier (artificial SEI film) is pre-constructed in the Na||graphite batteries to solve these thorny problems. With the CSMG (covered SEI on modified graphite), batteries deliver higher capacity 40 mAh/g even under the current density of 300 mA/g and the capacity retention maintains very well after 100 cycles at a high operating voltage. Moreover, the function mechanism was revealed by *in-situ* XRD, demonstrating that the pre-constructed SEI can effectively suppress the irreversible phase transition and exfoliation of graphite, resulting from the co-intercalation of anions. Additionally, the work voltage windows of carbonate electrolyte are significantly broadened by establishing electrode/electrolyte interphase. This method opens up an avenue for the practical application of DISBs on the grid energy storage and other fields.



Lithium-ion batteries (LIBs) have been widely used in portable electronics, electric vehicles and large scale energy storage for its high energy density, long-term stability [1]. With the development of society, the Ni-rich and Li-rich cathode materials have been attracted numerous attentions for their high theoretical energy densities [2,3]. While the transition metal Mn, Ni, Co resources are unevenly distributed, insufficient reserves on the earth, thus the price are more and more expensive [4,5]. With carbonaceous material as cathode, the dual ions batteries (DIBs) are expected to be the rising star in the future energy storage due to free transition metal, low cost and environmental friendliness [6–8]. Especially for dual ions sodium batteries (DISBs), the sodium resources are abundant and cheaper than the lithium metal. Moreover, the higher operating voltage (> 4.5 V *vs.* $Li^+$/Li) of DISBs can effective improve the power density and facilitate anions insert into the graphite layer reversibly [9]. Nevertheless, high operating voltage is a double-edged sword, leading to electrolyte decomposition, rapid capacity decay and low Coulombic efficiency [10]. Additionally, solvents are prone to co-intercalate into interlayers of graphite accompanied with anions during the process of charge, causing serious exfoliation and collapse of the cathode structure. These main challenges impede practical implementations of DISBs.

Tremendous efforts have been devoted to solving aforementioned problems. Different from the LIBs and sodium-ion batteries (SIBs), electrolytes are more important for DIBs' performances (energy density, cycle stability and nano-structural long-term stability). Owing that it not only acts as the transportation medium for ions mobility, cations and anions also participate the (de)insertion processes serving as active materials [11,12]. Thus optimizing electrolyte becomes the ideal choice to improve the performance of DIBs [13–16], such as introducing additives, adopting solvents with high oxidation tolerance or high concentration electrolytes, ionic liquids. With 5 mol/kg KFSI/EC/DMC concentrated electrolyte, the energy density of potassium DIBs were elevated to 270 Wh/kg, which is much higher than potassium DIBs with traditional electrolytes (20–70 Wh/kg) [17]. Moreover, the cycle stability and rate performance were greatly improved, originating from better electrolyte/electrode interphase and unique solvation structure.

* Corresponding authors.
*E-mail addresses:* daidongmei@htu.edu.cn (D. Dai), jiamengmin@htu.edu.cn (M. Jia), liudaihuo@htu.edu.cn (D.-H. Liu).

https://doi.org/10.1016/j.cclet.2022.107832
1001-8417/

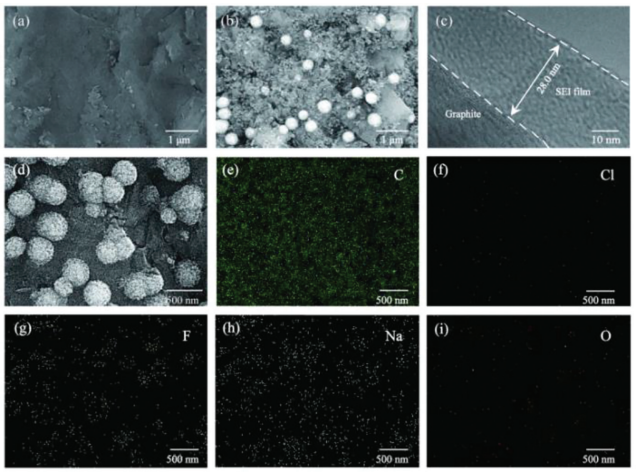


**Fig. 1.** (a) The SEM image of graphite electrode without pretreatment. (b) SEM and (c) TEM images of graphite after 5 cycles. (d-i) The SEM and corresponding elemental mapping images of graphite electrode after 5 cycles.

Besides, Cui *et al.* designed "anion-permselective" polymer electrolyte to weaken the interactions of anions and solvents, thus the behavior of anions co-intercalation were significantly inhibited [18]. Even under the high cut-off voltage 5.4 V, capacity retention of graphite||Li batteries is over 87% after 2000 cycles, while capacity of the one without using "anion-permselective" polymer electrolyte sharply drops to 0 mAh/g after 800 cycles.

The solid electrolyte interphase (SEI) film is crucial for the cycle stability, which acts as physical barrier to avoid the direct contacts of electrolyte and electrode [19]. Then the effective operating voltage ranges can also be broaden and the side reactions on the electrode/electrolyte interphase were also significantly reduced [20,21]. In addition, ions need to experience the process of desolvation before passing through the SEI, thus the co-intercalation and oxidation reactions of solvents can be solved at the same time [22,23].

Inspired by the positive role of SEI in the electrode/electrolyte interphase, we pre-constructed solid electrolyte interphase (SEI) layer in graphite half battery with film forming solvents ethylene carbonate (EC) [24,25] and fluoroethylene carbonate (FEC) [26], which significantly improves the cycle performance and the structural integrity of graphite cathode. DISBs with the artificial SEI can deliver higher capacity even under a high current density of 300 mA/g and the long-term cycle stability will be greatly improved at high cut-off voltage of 4.6 V, which is beyond the stable voltage range of the carbonate electrolyte. It indicates that pre-constructed SEI was built successfully and it broaden the operating voltage window [27,28]. On the contrary, capacity of the one without pre-constructed SEI declined faster, and the Coulombic efficiency is lower. Then the function mechanism of *ex-situ* SEI was deeply analyzed by *in-situ* XRD, which further verifies that the pre-constructed SEI can protect the graphite cathode from exfoliation. Furthermore, co-insertion of solvents and the side reactions were greatly reduced. Thus DISBs with artificial SEI show better long-term stability, rate performance and higher theoretical energy density. The method of pre-built SEI provides more possibilities for the practical application of dual ion battery.

As shown in Fig. S1 (Supporting information), the artificial SEI film on graphite cathode was prepared by charging/discharging in Na||graphite half batteries for several cycles with different electrolytes and various current densities at the range of 0.1–1.8 V (*vs.* $Na^+/Na$). Then the SEI films were characterized by SEM and TEM. As illustrated in Fig. 1, the graphite electrode without treatment was smooth, while after 5 charge/discharge the one became rough and some particles deposited on the electrode surface unevenly. Moreover, the formation of artificial SEI was further confirmed by the TEM, suggesting that the SEI covered on the surface of graphite uniformly and the thickness is about 28 nm. Then the uniform distribution of elements of Na and F as exhibited in Figs. 1e-i characterized by energy-dispersive X-ray spectroscopy inferred that the main ingredient of SEI may include NaF.

As shown in Fig. S2 (Supporting information), the *ex-situ* XPS were executed to analyze the main components of SEI, demonstrating that the SEI mainly included NaF, $Na_2CO_3$, $ROCO_2Na$ derived from the decomposition of carbonate electrolyte and sodium salt [28–32]. In C 1s spectrum, peaks located at 289.45 eV are $Na_2CO_3$ and $ROCO_2Na$, the others are C-C (284.8 eV), C-O (286.1 eV), PVDF (291.4 eV). In O 1s spectrum, peaks located at 537.9, 534 and 532.5 eV are $ROCO_2Na$, C-OH, $Na_2CO_3$ respectively, which are in accordance with C 1s spectrum. Besides, peaks in F 1s and O 1s of Na-F (685.7, 1072.8 eV) and $CO_3^{2-}$ (1072.2 eV) confirmed the existence of NaF and $Na_2CO_3$ in SEI film. Additionally, SEI enriched NaF can mitigate the oxidative reaction of electrolyte at high voltage and significantly inhibits volume expansion of graphite layers during repeated charge/discharge [33,34]. While the main components of UCMG (uncovering SEI on modified graphite) surface are active materials, conductive agent and binder. In additionally, electrodes were soaked in electrolyte and assembled as batteries rested for 12 h, respectively, then they were tested by XPS, which can be seen in Fig. S3 (Supporting information). After 12 h immersion in electrolyte, a single peak of C-F exists. There are two peaks of NaF and C-F for the electrode rested in cell for 12 h, but Na-F peak is quite weak. And the peak C-F derived from binder PVDF. Therefore, these results unveiled that the valid SEI only can be formed through the designed electrochemistry processes.

In order to analysis the amount of SEI film, TGA tests were further conducted. And the main single ingredient of graphite electrode was also tested under $N_2$ atmosphere from room temperature to 900 °C. As illustrated in Fig. S4 (Supporting information), the UCMG began loss weight from about 400 °C, which corresponds to the decomposition of PVDF, while for CSMG loss weight from the beginning, indicating that the decomposition of the main components of SEI formed on the surface of electrode. For the well thermostability of conductive agent and active material, they did not decompose within this temperature ranges. Thus the coverage amount of pre-constructed SEI formed on the graphite surface is about 4 wt%.

In order to optimize the conditions of SEI film formation, long-term performance of batteries with SEI formed under various conditions of different cycle numbers, current densities and electrolytes were tested. Firstly, it can be seen that batteries with SEI formed after 5 charge/discharge cycles in Fig. S5a (Supporting information), which shows higher discharge capacity of 75 mAh/g among four contrast samples, which higher than the ones of 1, 10, 20 cycles, respectively. Then the conditions of different current densities were further screened. Though long-term performances with various current densities are similar, the cycle stability and Coulombic efficiency of the one with 10 mA/g are much better, which possesses a high capacity and capacity retention (Fig. S5b in Supporting information). Afterwards, the performances of batteries with different SEI films formed with kinds of electrolytes were further compared. From the comparison, it can elucidate that the SEI formed in Na||graphite with electrolyte of 1 mol/L $NaClO_4$ in EC/DMC/EMC showed favorable performance in DISBs, whose initial capacity is about 45.5 mAh/g. While others with electrolytes of 1 mol/L $NaClO_4$ in EC/PC and 1 mol/L $NaClO_4$ in EC/DEC delivered lower capacity of 18.8 mAh/g and 21 mAh/g, respectively.

To further verify the effectiveness of artificial SEI, the rate performance and long-term performance of DISBs with electrolyte of 1 mol/L $NaClO_4$ in EC/DMC/EMC + 5 wt% FEC were investigated by adopting optimized conditions at the range of 0.6–4.6 V.

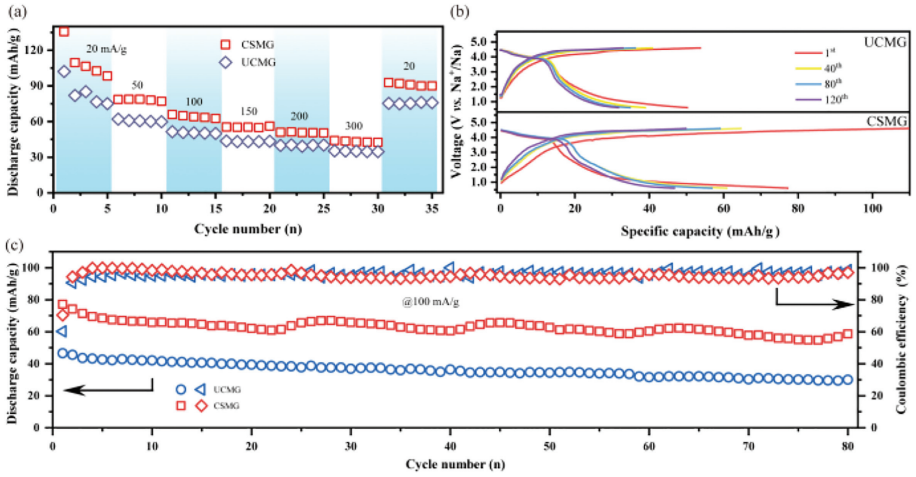


**Fig. 2.** Electrochemical performance of DISBs with UCMG and CSMG, (a) rate performance, (b) charge/discharge profiles, (c) long-term cycle performance.

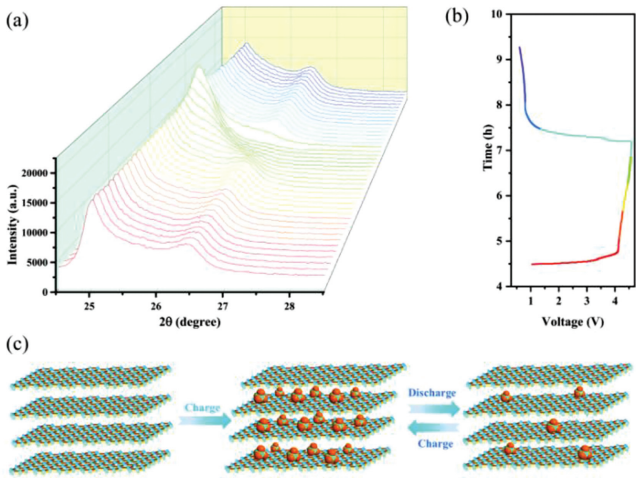


**Fig. 3.** The intercalation mechanisms of anions in CSMG cathode: (a) *In-situ* XRD pattern contour and (b) corresponding charge/discharge profiles of CSMG in DISBs. (c) The evolutions of intercalation chemistry of anions in CSMG during the charge/discharge processes.

As displayed in Fig. 2a, DISBs with CSMG showed better rate performance. Even under the high current density of 300 mA/g, the capacity of battery can still deliver > 40 mAh/g. While the one with UCMG exhibited lower capacity. It suggests that the artificial SEI covered on the graphite cathode did not affect the reaction kinetic. Besides, the capacity recovered very well after the current of battery with CSMG returns to the initial small current density, indicating that batteries with CSMG exihibits exceptional reversibility. As shown in Figs. 2b and c, batteries with CSMG show well long-term cycle stability and low over-potential voltage. Moreover, the charge/discharge profiles overlapped very well (Fig. 2b), which demonstrates that preformed SEI film can avoid solvent co-inserting accompanied with anions. Thus the side reaction and structure deterioration would be significantly eliminated by the SEI layer.

Additionally, after 5 cycles' formation in the Na||graphite batteries, the graphite electrodes were took out to assemble DISBs for deeply understanding the intercalation/de-intercalation processes of anions by *in-situ* XRD equipment. Then the second cycle's XRD pattern and charge/discharge profiles are exhibited in Fig. 3. After one cycle's charge/discharge, the main peak (002) located at 26.36° completely vanished and splitted into two peaks, suggesting that some intercalated anions remain in the graphite layers [35]. Thus the expansionary interlayer is favor to the fast anion (de)intercalation, leading to faster reaction kinetic. During the second cycle's charge/discharge processes, the splitted peaks gradually deviated from the center then returned to the initial state, which obviously demonstrates that batteries with CSMG electrodes show well reversibility during charge/discharge processes [36].

Then the EISs and SEM were conducted to study the interphase of electrode/electrolyte. As shown in Figs. S6a and b (Supporting information), electrode with CSMG exhibited larger impedance than the one with UCMG before cycling, indicating that the SEI film successfully formed on the graphite. After 80 cycles, the impedance of electrode with UCMG almost increases to 1200 Ω, which is nearly 3 times of the fresh electrode. On the contrast, the impedance of electrode with CSMG is nearly steady without obvious increase, indicating that the pre-constructed SEI layer can inhibit the side reactions of electrolyte under high voltage and avoid the accumulations of by-products. Thus a stable electrode/electrolyte interphase was constructed by artificial SEI layer. Figs. S6c and d (Supporting information) unravel the equivalent circuit for EIS spectra of UCMG and CSMG before cycling, in which $R_e$ represents the resistance of electrolyte and ohmic resistance, $R_l$ the leakage associated with electrode reaction in bulk electrode, $R_{ct}$ charge transfer resistance, and $R_{SEI}$ the SEI resistance, while $CPE_l$, $CPE_{ct}$ and $CPE_{SEI}$ are the corresponding capacitance. Moreover, the SEI layer can avoid solvation co-inserting into graphite layer, thus keeping the structure integrity of graphite electrode [37,38]. In additionally, after 80 cycles batteries with CSMG and UCMG were disassembled, then the surface morphology of electrodes were observed by SEM. As illustrated in Figs. S6e and f (Supporting information), the surface of CSMG is still rougher than that UCMG, indicating that the preformed SEI is still existence. The EISs and SEM images further prove that the artificial SEI layer can effective protect the graphite from structure disorganizing and reduce the oxidative decomposition of electrolytes on the electrolyte/electrode interphase, which enables long-term stable cycle performance [39].

Fig. 4 illustrates the mechanism of DISBs with pre-constructed SEI films, demonstrating that the operating voltage can be effectively broaden by the artificial SEI. Then the decompositions of carbonate electrolyte are greatly inhibited, reducing the accumulations of by-products and improving the Coulombic efficiency as well as cycle stability. As shown in Fig. 4, $ClO_4^-$ anions migrate to the graphite cathode and insert into the graphite layer during charging, while $Na^+$ cations move to the sodium anode and

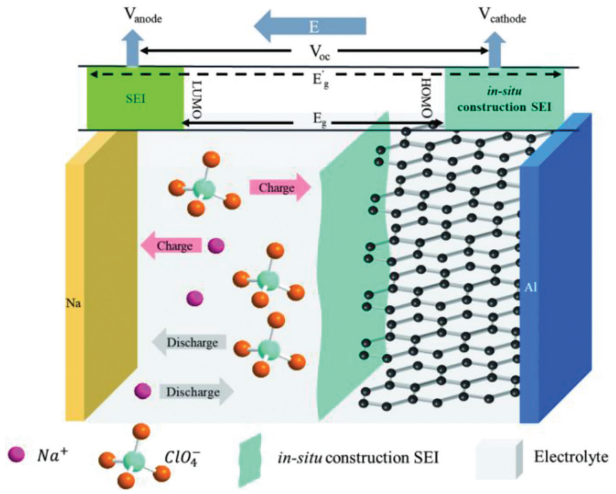


**Fig. 4.** Mechanism of DISBs with pre-constructed SEI films.

deposit on the surface of sodium. Then during discharge processes, the $ClO_4^-$ anions inserted into the graphite layers and the $Na^+$ deposited on the anodereturn back to the electrolyte. In general, the electrochemical stable voltage window of DISB should be limited within the highest occupied molecular orbital (HOMO) and Lowest Unoccupied Molecular Orbital (LUMO) of the electrolyte, otherwise the electrolyte will easily decompose if the voltage is too high. The pre-constructed SEI on the surface of the graphite cathode can effectively inhibit the electrolyte decomposition and improve electrolyte stability from $E_g$ to $E'_g$. Therefore, the performance of the battery with pre-constructed SEI is desirable in a wide voltage window. Additionally, with the artificial SEI as physical protector, the co-insertions of solvents can also be avoided during the process of $ClO_4^-$ (de)insertion. Then the structure of graphite cathode can be maintained very well after long-term cycles.

In short, the long-term cycle stability and rate performance of graphite based dual ion sodium batteries were significantly improved *via* pre-constructed SEI. With the deeply understanding by *in-situ* XRD and electrochemical performance, we found that the artificial SEI plays an important role in the DISBs system. It can not only serve as physical barrier that avoids the direct contact of electrode and electrolyte, avoiding the oxidative decomposition of carbonate electrolytes; but also can impedes solvents co-insertion into graphite, reducing the exfoliation of graphite cathode. Under the protection of artificial SEI, the capacity retention of DISBs with CSMG is 76% after 80 cycles, which is higher than that one with UCMG (64%). In addition, with the enriched NaF SEI, batteries with CSMG display better rate performances, demonstrating that the charge/discharge kinetics of DISB are improved for the enriched NaF. This work shed light on the DISBs practical applications under high operating voltage.

## Declaration of competing interest

The authors declare that they have no known competing financial interests or personal relationships that could have appeared to influence the work reported in this paper. All the authors have given their consent for submission of this manuscript.

## Acknowledgments

This work was financially supported by the National Natural Science Foundation of China (Nos. 51672071, 51802085, 51772296 and 51902090), "111″ Project (No. D17007), the National students' platform for innovation and entrepreneurship training program (No. 201910476010), the China Postdoctoral Science Foundation (No. 2019 M652546), and the Henan Province Postdoctoral Start-Up Foundation (No. 1901017).

## Supplementary materials

Supplementary material associated with this article can be found, in the online version, at doi:10.1016/j.cclet.2022.107832.

## References

[1] M. Li, J. Lu, Z.W. Chen, K. Amine, Adv. Mater. 30 (2018) 1800561.
[2] N.F. Hu, C. Zhang, K.F. Song, et al., Chem. Eng. J. 415 (2021) 129042.
[3] W. Liu, P. Oh, X. Liu, et al., Angew. Chem. Int. Ed. 54 (2015) 4440–4457.
[4] R. Schmuch, R. Wagner, G. Horpel, T. Placke, M. Winter, Nat. Energy 3 (2018) 267–278.
[5] M.M. Thackeray, K. Amine, Nat. Energy 6 (2021) 933-933.
[6] Q. Liu, Y.Z. Wang, X. Yang, et al., Chem 7 (2021) 1993–2021.
[7] Y.M. Sui, C.F. Liu, R.C. Masse, et al., Energy Storage Mater. 25 (2020) 1–32.
[8] J. Liu, Y. Zhao, X. Huang, et al., Chem. Eng. J. 435 (2022) 134839.
[9] X.L. Zhou, Q.R. Liu, C.L. Jiang, et al., Angew. Chem. Int. Ed. 59 (2020) 3802–3832.
[10] X.W. Ou, D.C. Gong, C.J. Han, Z. Liu, Y.B. Tang, Adv. Energy Mater. 11 (2021) 2102498.
[11] K.V. Kraychyk, P. Bhauriyal, L. Piveteau, et al., Nat. Commun. 9 (2018) 4469.
[12] X. Wang, S. Wang, K. Shen, et al., J. Mater. Chem. A 8 (2020) 4007–4016.
[13] H.Z. Jiang, X.Q. Han, X.F. Du, et al., Adv. Mater. 34 (2022) 2108665.
[14] K. Duan, J. Ning, L. Zhou, et al., ACS App. Mater. Interfaces 14 (2022) 10447–10456.
[15] J. Liu, X. Song, L. Zhou, et al., Nano Energy 46 (2018) 404–414.
[16] J. Ning, K. Duan, K. Wang, et al., J. Energy Chem. 67 (2022) 290–299.
[17] A.P. Wang, S. Kadam, H. Li, S.Q. Shi, Y. Qi, Npj Comput. Mater. 4 (2018) 15.
[18] D. Diddens, W.A. Appiah, Y. Mabrouk, et al., Adv. Mater. Interfaces 9 (2022) 2101734.
[19] P. Peljo, H.H. Girault, Energ. Environ. Sci. 11 (2018) 2306–2309.
[20] H.R. Cheng, Q.J. Sun, L.L. Li, et al., ACS Energy Lett. 7 (2022) 490–513.
[21] I.A. Rodriguez-Perez, X. Ji, ACS Energy Lett. 2 (2017) 1762–1770.
[22] H.H. Zheng, G. Liu, V. Battaglia, J. Phys. Chem. C 114 (2010) 6182–6189.
[23] H.Y. Liang, X.X. Zuo, L.D. Zhang, et al., J. Electrochem. Soc. 167 (2020) 090520.
[24] X. Zhou, P. Li, Z.H. Tang, et al., Energies 14 (2021) 7467.
[25] J.B. Goodenough, K.S. Park, J. Am. Chem. Soc. 135 (2013) 1167–1176.
[26] J.B. Goodenough, Y. Kim, Chem. Mater. 22 (2010) 587–603.
[27] A. Andersson, K. Edström, J. Electrochem. Soc. 148 (2001) A1100.
[28] V. Eshkenazi, E. Peled, L. Burstein, D. Golodnitsky, Solid State Ion. 170 (2004) 83–91.
[29] M. Lu, H. Cheng, Y. Yang, Electrochim. Acta 53 (2008) 3539–3546.
[30] P. Verma, P. Maire, P. Novák, Electrochim. Acta 55 (2010) 6332–6341.
[31] K. Edström, M. Herstedt, D.P. Abraham, J. Power Sources 153 (2006) 380–384.
[32] D.D. Yu, Q.N. Zhu, L.W. Cheng, et al., ACS Energy Lett. 6 (2021) 949–958.
[33] D.Y. Wang, C.Y. Wei, M.C. Lin, et al., Nat. Commun. 8 (2017) 14283.
[34] X. Wang, M. Hou, Z. Shi, et al., ACS App. Mater. Interfaces 13 (2021) 12059–12068.
[35] Z.D. Huang, Y. Hou, T.R. Wang, et al., Nat. Commun. 12 (2021) 3106.
[36] K. Xu, A. von Wald Cresce, J. Mater. Res. 27 (2012) 2327–2341.
[37] K. Xu, J. Electrochem. Soc. 154 (2007) A162.
[38] X.B. Cheng, C.Z. Zhao, Y.X. Yao, H. Liu, Q. Zhang, Chem 5 (2019) 74–96.
[39] W.H. Li, Q.L. Ning, X.T. Xi, et al., Adv. Mater. 31 (2019) 1804766.